ESD-TR-86-005

Project Report
ETS-77

Calibration of ETS Videotapes

A.J. Yakutis
L.G. Taff
S. Sayer

29 April 1986

Lincoln Laboratory

MASSACHUSETTS INSTITUTE OF TECHNOLOGY

LEXINGTON, MASSACHUSETTS

Prepared for the Department of the Air Force
under Electronic Systems Division Contract F19628-85-C-0002.

The work reported in this document was performed at Lincoln Laboratory, a center for research operated by Massachusetts Institute of Technology, with the support of the Department of the Air Force under Contract F19628-85-C-0002.

Thomas J. Alpert, Major, USAF
Chief, ESD Lincoln Laboratory Project Office

MASSACHUSETTS INSTITUTE OF TECHNOLOGY
LINCOLN LABORATORY

CALIBRATION OF ETS VIDEOTAPES

A.J. YAKUTIS

L.G. TAFF

S. SAYER

Group 94

PROJECT REPORT ETS-77

29 APRIL 1986

LEXINGTON MASSACHUSETTS

ABSTRACT

This Project Report discusses an attempt to calibrate photometric data acquired from streaks generated by moving objects which were observed at the ETS. This is desirable for both natural and artificial bodies. The utility of a meaningful apparent magnitude from streak data would allow statistical studies of size-albedo distributions, serve as a size indicator in the absence of traditional photometry, and alleviate the difficulties of artificial satellite photometry on the rapidly moving near-Earth population. Unfortunately we have been unsuccessful at this endeavor. Moreover, were this trial successful we can envisage sundry systematic errors that would creep into more widespread applications. Some of these are related to angular speed, field of view, time duration of a streak, frame-to-frame variability, length of streak arc across the field of view, and the angle between the angular velocity and the direction of the video scan lines. This general topic is important and we will pursue other approaches if they can address our apprehensions.

TABLE OF CONTENTS

LIST OF ILLUSTRATIONS

LIST OF TABLES

CALIBRATION OF ETS VIDEOTAPES

I. INTRODUCTION

The ETS primarily observes objects that move — artificial satellites and meteors near the Earth and minor planets farther away from the Earth. Many of the detection, discrimination, and recording mechanisms at the observatory rely on this motion to produce a streak (or streak-like effect). It would be useful in many situations to be able to reconstruct a meaningful apparent magnitude from such a streak. We have attempted to do this, in a variety of ways, several times in the last year. All resulted in failure. This report details our most recent, and sophisticated, failure. Because we are prepared to argue that this should have worked, and it did not, we are forced to conclude that it is useless to further pursue this endeavor. However, we would greatly appreciate constructive criticism that will help us overturn our pessimistic conclusion.

We have tried to calibrate the brightness of streaks caused by moving bodies by utilizing streaks of stars. The stars are of known brightness and color. Stellar streaks were created by driving the telescope at a known angular velocity through the star field. The star selection, calibration, photometric measurements, and so on are all detailed below for "static star" measurements. Similarly, we discuss the slightly different methods used for "star streak heads" and "streaking stars" too. Angular speed dependence is not discussed for we feel that from the quality of our current data, there is no point in doing so. Systematic errors owing to the position angle of the angular velocity are briefly outlined. These have the potential to dominate all other uncorrectable error terms.

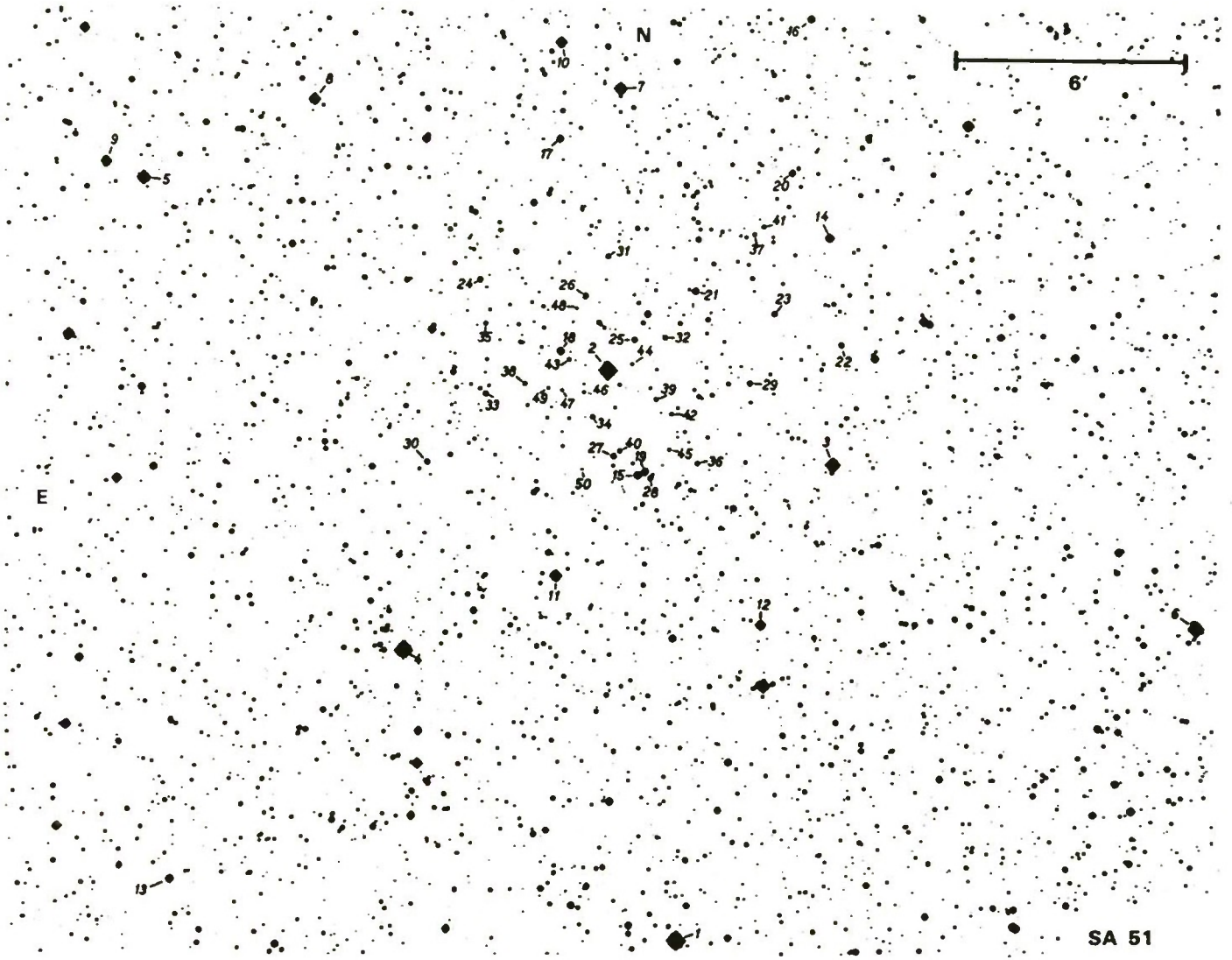

Figure 1. The finding chart from Purgathofer (1969) for SA51. Note that the plate scale indicator is incorrect and that it should be 10!7.

II. OBSERVING PROCEDURES

We wanted a small area of the celestial sphere with a reasonable stellar density. Moreover, we wanted a significant fraction of the stars in the field to have multicolor photometry. These data are required so that we may transform standard astronomical photometry into the natural system of the camera, i.e., the S-20 photocathode response. Clusters of stars, of which hundreds exist with excellent multicolor photometry, generally are too dense. (We were looking ahead to streaks and crowding would be a severe problem in the fields of most galactic or globular clusters.) Hence, we settled on a Selected Area of Kapetyn, in particular number 51. Figure 1 shows the central part of SA51 from Purgathofer's (1969) finding chart.* Note that the indicated plate scale is incorrect; a better value is 10!7.

Static star data consist of several minutes of videotaped data of this field with the telescope (we used the A telescope) in sidereal drive. At a one-thirtieth of a second refresh rate, we have a multitude of video frames to choose from. We used four. This is enough to show both the existence of frame-to-frame variability and to start to quantify it.

The cameras used for this work are the standard intensified EBSICON devices that have been in use at the ETS for several years. The videotape recorder is a SONY Corporation Model 5850. Streaking star data consist of several frames of videotaped data of this field with the telescope moving at the sidereal rate in right ascension and some arbitrary rate in declination. Data were acquired from 0-3600″/s in 300″/s steps. The telescope was always moving northward. The data discussed herein are the 1500″/s = 0°42/s set.

Finally, a series of measurements of the camera's sensitivity were also made. A single star ($V = 14^{m}.4$) was placed at 64 equally spaced points across the camera target. At each of these grid locations a signal-to-noise measurement was made. These values were used to correct for responsivity variations in the camera target. Figure 2 shows a rough isophotal contour map of these nonuniformities.

All the data were acquired for us by D.E. Beatty and R.C. Ramsey. We wish to acknowledge their contribution and express our thanks.

* A.Th. Purgathofer, Lowell Obs. Bull. No. 147, 7, 10 (1969).

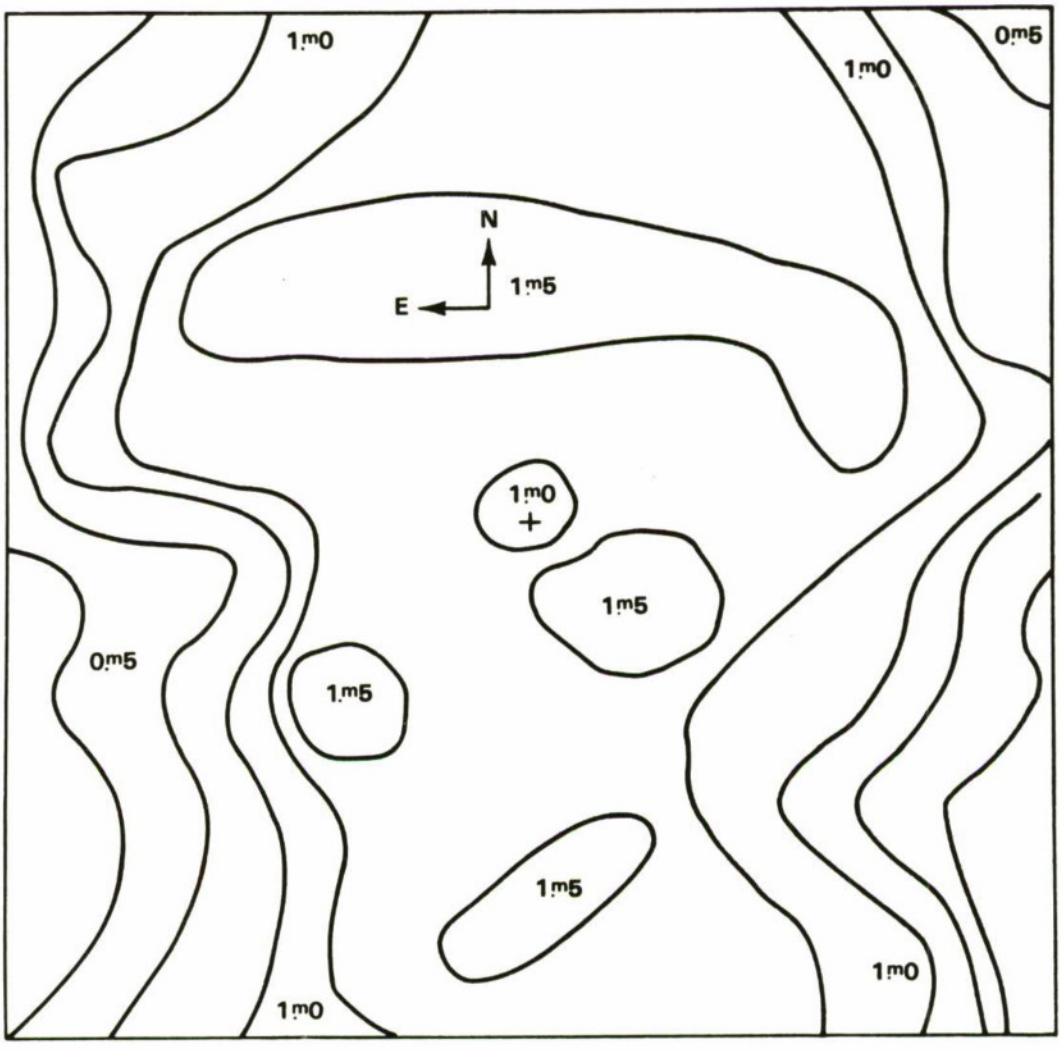

73765-6

Figure 2. Isophotal contour map of the variations in the camera target's sensitivity.

III. DATA ACQUISITION

A. Static Stars

Presumably some measure of the total intensity of a star's image on a small area of the camera target is related to its photometrically determined apparent magnitude. As the wavelength response of the camera target follows the S-20 photocathode variation, the natural apparent magnitude to attempt to mimic is m_{20}. By utilizing the V and B-V data for SA51 in Purgathofer (1969) and Sorvari's (1977) transformation equation,* we can convert V and B into m_{20}. The formula is

$$m_{20} = V - 0^m.38 + 0.61(B - V)$$

The total intensity level was measured with an Interactive Video Systems digital image processor model number 210. One of the capabilities of this machine is the following: A rectangular box of (nearly) arbitrary dimensions can be placed at a random location in the field of view. At the push of a button the device prints out a histogram of the intensity levels of the elementary picture elements within the box. The IVS machine has a 512×480 column $\times$ row format. Typical static star box sizes are 5×7 and 6×8. The largest box was 15×16 in size. Theoretically using a box too large ensures that all the starlight is counted but it requires a larger background correction in practice.

The background level was ascertained by placing the IVS box as near as possible to the star's location and obtaining a new intensity histogram. Naturally our ability to juxtapose the star's box and the background box is limited by crowding (from other stars) and contamination by scintillations. The IVS measurement is itself repeatable and error-free.

The end product of these three steps is an S-20 apparent magnitude for each star, an array that we denote by $N_s(n)$, $n = 0,1,2,...,N_{max}$, which contains the stellar box intensity level histogram, and an array $N_b(n)$ for the background box. In addition, we know the locations of the IVS boxes on the camera target. (N_{max} is the maximum meaningful intensity level and corresponds to just saturating the camera target for the brightest star in the field.)

B. Star Streak Heads

The method of data reduction for star streak heads is identical to that for static stars. By "star streak head" we mean the leading edge of the streak. The majority of the streak itself, that is the tail, is the result of lag effects in the camera. Although the camera specifications are quite explicit as to the amplitude and duration of the lag, we thought it best to attempt to isolate the head of the streak before dealing with the entire streak.

---

* J.M. Sorvari, "Magnitudes of Stars on the S-20 System," Project Report ETS-19, Lincoln Laboratory, M.I.T. (14 September 1977), DDC AD-A047099/7.

The principal danger in making these measurements is that the star streak head box will be larger than the streak head itself thereby including part of the tail. As this potential pitfall will include the brightest part of the tail, the effect should be most noticeable for the brightest stars. It turned out to be so and data obtained on them were obviously contaminated. Box sizes for this phase were slightly larger than those used for the measurements of the same star in the static mode.

C. Streaking Stars

In principle the method of data reduction for streaking stars is identical to that for static stars. The practical difference is that streaks occupy a much larger area on the camera target than static stars do. Therefore, a single correction for background level or camera sensitivity would be inappropriate. Moreover, while the edges of static stars are fairly clear to the eye, the merging of streaks with the background is not. Indeed, some stars which are crystal clear in the static mode and in the streaking mode, become totally invisible when a particular frame of the streak is individually examined in the stop-frame (or pause) mode of the videotape recorders. (It is of course, the existence of the stop-frame capability that allows the measurement of streaking stars at all. The recorders can only hold a frame of video data for about 30 s — then they automatically release the videotape to prevent damage. We used the IVS-210 digital image processor to snatch the frames for longer-term playback.) Thus, we have "static star" data on some stars in SA51 for which we could not acquire "streaking star" data. As we have discussed before in this context, the aspect of motion when the videotapes are played at normal (or near-normal) rates plays a key role in the detection of the fainter streaks. Indeed, it is crucial beyond $m_{20} \simeq 15^m$.

In order to minimize undesirable systematic errors arising from nonuniform background or sensitivity variation corrections, we divided each streak into a series of vertical segments (see Figure 3). Competing with the desire to perform the corrections in an acceptable manner is the rapid growth of the computational load of doing so. We compromised by utilizing a box whose vertical extent was one-half of the calibration grid-point spacing. This turned out to be 30 units long. A uniform width of 8 was adopted. So for each streak we have two **sets** of pairs of N_{st}, N_b arrays. The number of pairs in a set varied with the brightness of the star and the particular frame being measured. Each streak array N_{st} can now be separately corrected for the local background via N_b and the local camera target nonuniformities via the same type of bivariate interpolation performed for the static stars.

In this vein of argument one might posit that the quantity to compare to m_{20} is not an apparent magnitude based upon one frame of a multi-frame streak but one based upon the summation of this kind of data from many (all?) frames of a multi-frame streak. The duration of a streak depends upon the object's topocentric angular velocity, the field of view of the telescope, and the telescope's inertial angular velocity. While we can simply control the latter two variables — and make them uniform for all data collection — the former varies over three orders of magnitude just covering the artificial satellite range. One might be able to develop a formula that related angular speed to the number of frames included in the summation. We do not believe

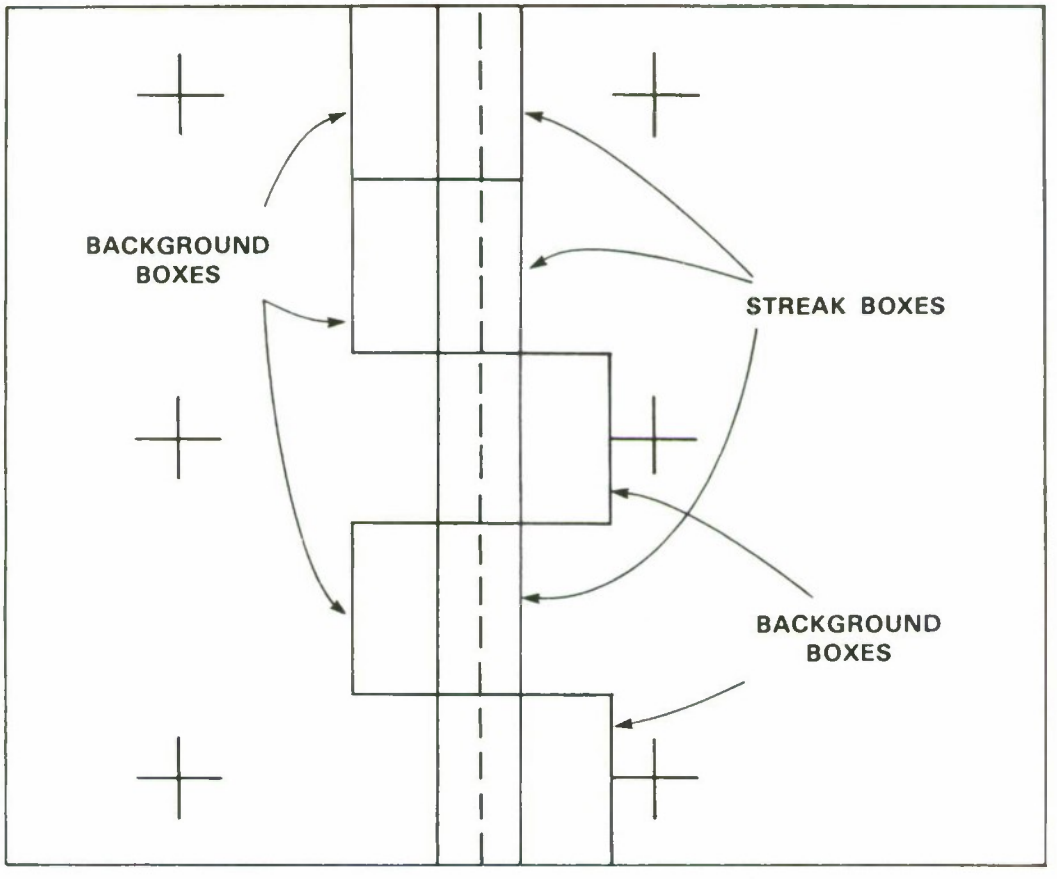

Figure 3. Schematic diagram of IVS-210 box location along a streak. The plus signs denote locations where the camera target sensitivity is known.

that an adequate correction for the position angle of the angular velocity (see Figure 4) can be made. A correction for frame-to-frame variability would clearly be necessary too and we cannot envisage the successful completion of this task (see below). Finally, the computational effort will grow extraordinarily rapidly as multiple sets of N_{st} and N_b arrays are reduced for each of 5 (10?) frames.

D. Frame-to-Frame Variations

The above descriptions for static and streaking stars implicitly discuss the reduction of data for a single video frame. We do not know, *a priori*, what the amplitude of the frame-to-frame variations might be. We would predict that they could be very large for streaking stars. Hence, everything described above was performed several times for the static stars, the star streak heads, and the streaking stars. When the static star data are reduced the frame-to-frame variations seen in it represent the minimum values that will exist in the streaking star data. They turn out to be $0^m.5$ and, therefore, unacceptably large.

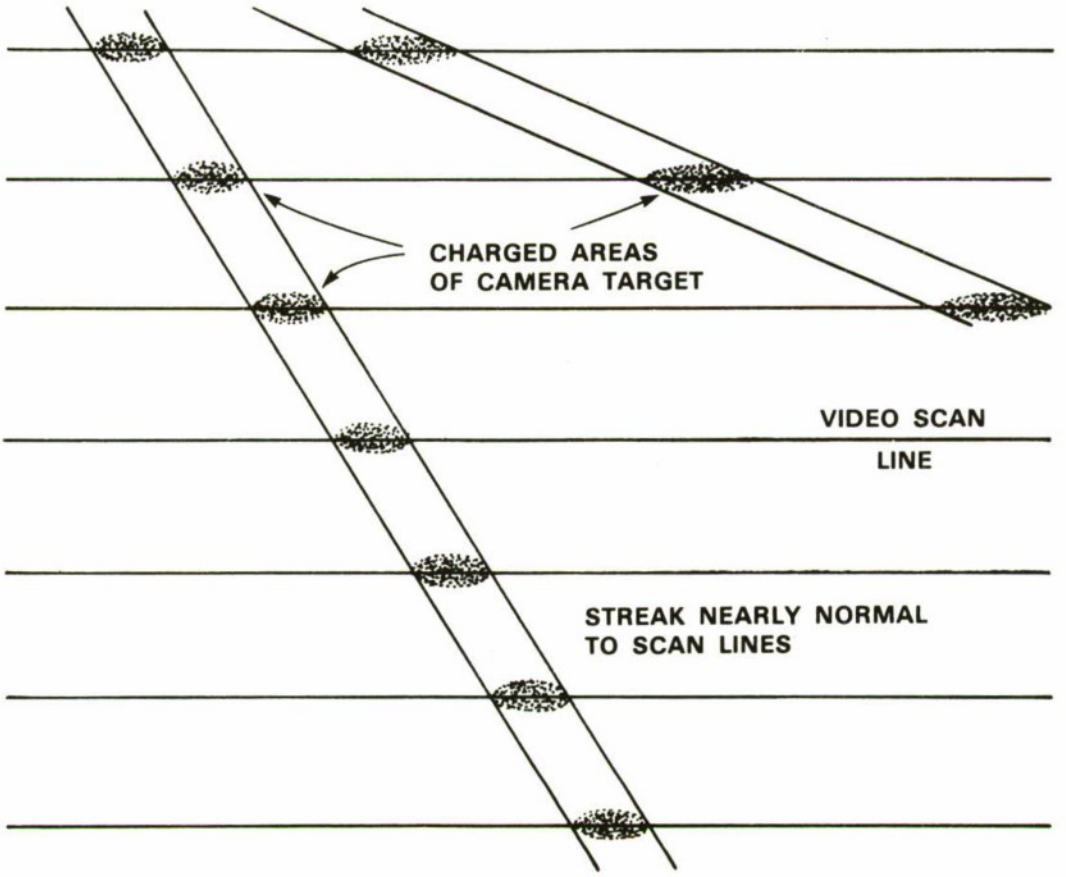

Figure 4. Exaggerated view of a few video scan lines and two streaks. As the streak becomes more nearly parallel to the scan line direction it may fall between scan lines thereby implying that it is fainter than it is.

IV. COMPUTATIONS

A. Static Stars

For each static star measurement form

$$l_s = \sum_{n=0}^{N_{max}} nN_s(n) \tag{1}$$

and

$$I_b = \sum_{n=0}^{N_{max}} nN_b(n) \tag{2}$$

The uncorrected S-20 apparent magnitude is defined to be

$$m' = c - 2.5 \log(I_s - I_b) \tag{3}$$

for some unknown constant c. Note that the (in this case almost uniform) extinction correction is buried in c. The corrected (for camera target sensitivity variations) S-20 apparent magnitude is given by

$$m = m' + \Delta m \tag{4}$$

The quantity Δm represents the result of a bivariate linear interpolation amongst the appropriate set of four signal-to-noise measurements from our 64-point calibration grid. It provides the camera target sensitivity variation correction relative to an arbitrary level. Note that l_s and l_b are not separately adjusted. The reason is that the static star boxes are either comparable (in width) or much smaller (in height) than the standard 8×30 streaking star box. Having given up sensitivity variation resolution below 30 pixels for the more difficult case of streaking stars, a refinement of this nature here seems superfluous. A second systematic error introduced at this stage is to assume that the logarithm of the average is equal to the average of the logarithms. We do not believe that either of these can materially affect the overall quality of our results nor can they have led us to an overly pessimistic conclusion. Finally, should others choose not to deliberately make these errors, the proper method of reduction is clear (albeit computationally burdensome).

The sign of Δm in Equation (4) is easily predicted. When a star in SA51 fell on a place of the camera target which was relatively insensitive, then l_s and I_b in Equations (1) and (2) are too low. Therefore m′ will be larger (algebraically) than it should be because the star will appear to be fainter than it is; see Equation (3) and the minus sign before the logarithm. Hence, in such an area of the camera target, Δm is less than zero. Conversely, when a star in SA51 fell on a place of the camera target which was relatively supersensitive, then I_s and l_b are too high. Therefore m′ will be smaller than it should be because the star will appear to be brighter than it is. Hence, in such an area of the camera target, Δm is positive.

After all the N_s and N_b arrays are acquired, m′ calculated from them, and then corrected to m, we could then determine the nature of the relationship between m and m_{20}. Ideally it is

$$m = m_{20}$$

but in practice we utilized the stellar data, from each frame separately, to deduce the values of a and b in

$$m = am_{20} + b \tag{5}$$

We expect no color term because m_{20} is in the S-20 system and m is an inherently natural S-20 apparent magnitude. Color terms can arise from non-grey properties of the camera target or the telescope optics.

After each frame's data set is reduced we can examine the frame-to-frame variation in a and b. The frame-to-frame standard deviation in m is of the form

$$\sigma_{ff}^2 = \sigma_a^2 m_{20}^2 + \sigma_b^2$$

An important point is the fact that σ_{ff} increases with increasing m_{20}; this shows how a careful calibration on brighter stars will necessarily start to fail on fainter ones.

B. Star Streak Heads

The computations for star streak heads are identical in concept and execution as those for static stars. The inclusion of part of the tail in the case of the brightest stars vitiated the linear relationship in Equation (5) leading to their exclusion.

C. Streaking Stars

The computational sequence for streaking stars is similar to that for static stars; there are just more steps involved. For each pair of 8 × 30 streak and background box intensity histograms we computed an I_{st} and an I_b value [as in Equations (1) and (2)]. The next step was to compute an m′ and m (with the appropriate value of Δm) from Equations (3) and (4). m is not the apparent magnitude of the streak, merely the corrected apparent magnitude equivalent for this box of the streak (on the frame that it appears, ...). This value is converted back to an equivalent aggregate intensity level I_e. (We are informed that a common term for the quantities we are symbolizing by an I is "integrated optical density." If this adjectival phrase conveyed information we might promulgate it. As it does not, we refuse to.) Finally, the sum over all boxes for this streak of its equivalent aggregate intensity levels is utilized to calculate the corrected, S-20, apparent magnitude of the streak, viz.,

$$m_{st} = c - 2.5 \log\left(\sum_{\text{boxes}} I_e\right)$$

$$= -2.5 \log\left(\sum_{\text{boxes}} 10^{-0.4m}\right) \tag{6}$$

Like the static star multiple frame data, the m_{st} values could be fit to the corresponding m_{20} value as in Equation (5),

$$m_{st} = \alpha m_{20} + \beta \tag{7}$$

It is not, however, clear that the frame-to-frame differences in m_{st} are solely owing to video frame variations. The whole suite of systematic errors and calibration difficulties contributes to the spread in m_{st} values.

D. Systematic Errors

In the course of the above exposition we have described some potential sources of systematic error. There are other pitfalls which are mentioned below and some of the items already alluded to require a fuller treatment.

We have ignored color responsivity variations across the camera target — mainly because we did not think to investigate it. We also have no evidence that it is a minor effect. However, as the stars we used in SA51 have a typical range of B-V values, and variations in U are not readily detectable with an S-20 responsivity, unless the gradient of any color responsivity variation across the camera target is steep, it cannot affect our overall conclusions.

We have ignored differential extinction across the 0°5 field of view. This is clearly permissible for any reasonable air mass.

Had this calibration succeeded, then we would have had to face the question of the relativity of motion. Does it in fact make a difference if the telescope is fixed (i.e., in sidereal drive) and the object moves as opposed to the object being fixed while the telescope moves? We do not know.

We actually made the measurements of the streaks on images recorded in and played back through an IVS-210 digital image processor (see Section III-C). Does this mechanism introduce a noise problem? (Almost certainly yes). Is it random or systematic? (We hope that it is the latter and constant but if the former then small in amplitude.) Would we have to use the identical instrument (or just one of this model number) forever? (Probably.) What happens if a part is replaced? (At the best a new, small, systematic correction is introduced.) We could go on but instead we shall assume that our point is made.

We do not know the exact relationship between IVS-210 x-y coordinate values and the 64-point grid used for calibrating the signal-to-noise ratios. Naturally we made efforts to insure a proper alignment but neither the probability of a shift nor that of a rotation is zero. The net result for the static star data is to introduce a bias in each star's Δm value in Equation (4). This will not affect the estimate of frame-to-frame variability but will increase the scatter in a global fit to m_{20} values. The effects on streaking star data are similar but the summation in Equation (6) causes a complex interaction.

We have only acquired data on vertical streaks when the camera was properly aligned. That means that the streak direction is as close to being perpendicular to the camera scan line direction as we can arrange. Therefore, little signal is lost because the image is falling between scan lines. Obviously as the streak direction departs from the vertical this loss does occur, reaching a maximum for a horizontal streak midway between two scan lines. We have no estimate of the importance of this effect but it must be huge for fainter streaks unfortunately placed. We also have no way of correcting for it.

We have only examined one angular speed in any detail. It is reasonable to expect that α and β in Equation (7) are functions of angular speed, with a and b in Equation (5) as their limits, as $\omega \rightarrow 0$. If it made sense to pursue this work further, then a thorough exploration of α and β with ω would be necessary. Also, at high angular speeds the choice of a video frame to use is limited. Hence, if frame-to-frame variability is important, this variation cannot be adequately corrected for.

V. RESULTS

A. Static Stars

Table 1 lists the identification numbers, V, and B-V values of the stars in SA51 we used. Table 2 lists the values of a and b deduced from the measurement of four frames for static stars and those obtained by utilizing all the measures simultaneously in a least-squares fit. Two things are clear; a is nearly unity and b varies quite a bit. This variation represents fluctuations in the frame-to-frame zero point constant. Presumably this is telling us something about videotape or the camera as opposed to the sky, the telescope, or our measuring technique. With an amplitude difference of $0^m.6$ no serious photometry can be performed. A logical way to try and reduce the frame-to-frame variability is to signal average. Then we could measure the images of static stars with some smoothing of the background. Clearly this makes no sense for streaks so we never tried it.

TABLE 1

Standard Star Magnitudes

I.D. Number	V	B-V	m_{20}
3	$9^m.76$	$0^m.19$	$9^m.50$
4	9.81	1.04	10.06
11	10.75	1.05	11.01
12	10.96	0.58	10.93
15	11.67	0.38	11.52
18	12.16	1.12	12.46
19	12.25	0.71	12.30
23	12.81	0.55	12.77
24	12.88	0.74	12.95
25	13.13	0.63	13.13
27	13.28	1.01	13.52
28	13.50	0.26	13.28
34	14.08	0.65	14.10
39	14.73	0.63	14.73
42	15.20	0.91	15.38

TABLE 2

Least-Squares Parameters for Static Stars*

Frame Number	a	b	Residual
1	0.92	$-19^{m}.75$	$0^{m}.22$
2	0.85	-18.95	0.16
3	0.97	-20.26	0.18
4	0.90	-19.45	0.28
All	0.92	-19.69	0.22

* $m = am_{20} + b$

After obtaining these disappointing results we added a degree of freedom: Instead of forcing m to fit m_{20} we performed least-squares fits of the form

$$m = a + bV + c(B\text{-}V)$$

The results from these fits are in Table 3. The amplitude of the variation is comparable to that in Table 2 and the color terms are similar. [There is an obvious set of analytical relationships between a, b, and c in $m = a + bV + c(B\text{-}V)$ and the a and b in $m = am_{20} + b$ which turns out to be very well fulfilled numerically. Therefore, the formal aspects of an extra degree of freedom are not explored by the data. Perhaps the inclusion of a V-R term would be more appropriate.] Figure 5 shows a star-by-star and frame-by-frame plot of $m + 20$ vs m_{20}.

For reasons having to do with the chronology of assembling this report a second, independent set of 4 frames of static star data were acquired and analyzed. The a and b values corresponding to those in Table 2 ranged from 0.89 to 0.95 for a and from $-19^{m}.21$ to $-19^{m}.80$ for b. The residuals from the fit were also comparable, $0^{m}.23$ to $0^{m}.33$. (The values for the cumulative reduction were a = 0.92, b = $19^{m}.59$, root-mean-square residual = $0^{m}.24$ indicating, not surprisingly, the smoothing effects of averaging.) Similarly we have results comparable to those in Table 3 for a three parameter fit $-19^{m}.97 \geqslant a \geqslant -20^{m}.23$, $0.93 \leqslant b \leqslant 0.98$, $0.09 \leqslant c \leqslant 0.15$, with residuals ϵ $[0^{m}.17, 0^{m}.30]$. The results for a simultaneous reduction were a = $-20^{m}.00$, b = 0.96, c = 0.10, root-mean-square residual = $0^{m}.20$, very nearly equal to those in the bottom line of Table 3. Finally, the alternate version of Figure 5 that we could have included would exhibit the two principal features as shown by this Figure 5 (i.e., the linearity and the frame-to-frame variation).

TABLE 3

Least-Squares Parameters for Static Stars*

Frame Number	a	b	c	Residual
1	$-20^{m}.11$	0.95	0.12	$0^{m}.17$
2	-19.04	0.86	0.11	0.12
3	-20.63	0.98	0.28	0.16
4	-19.84	0.93	0.07	0.30
All	-20.01	0.94	0.14	0.17

* m = a + bV + c(B-V)

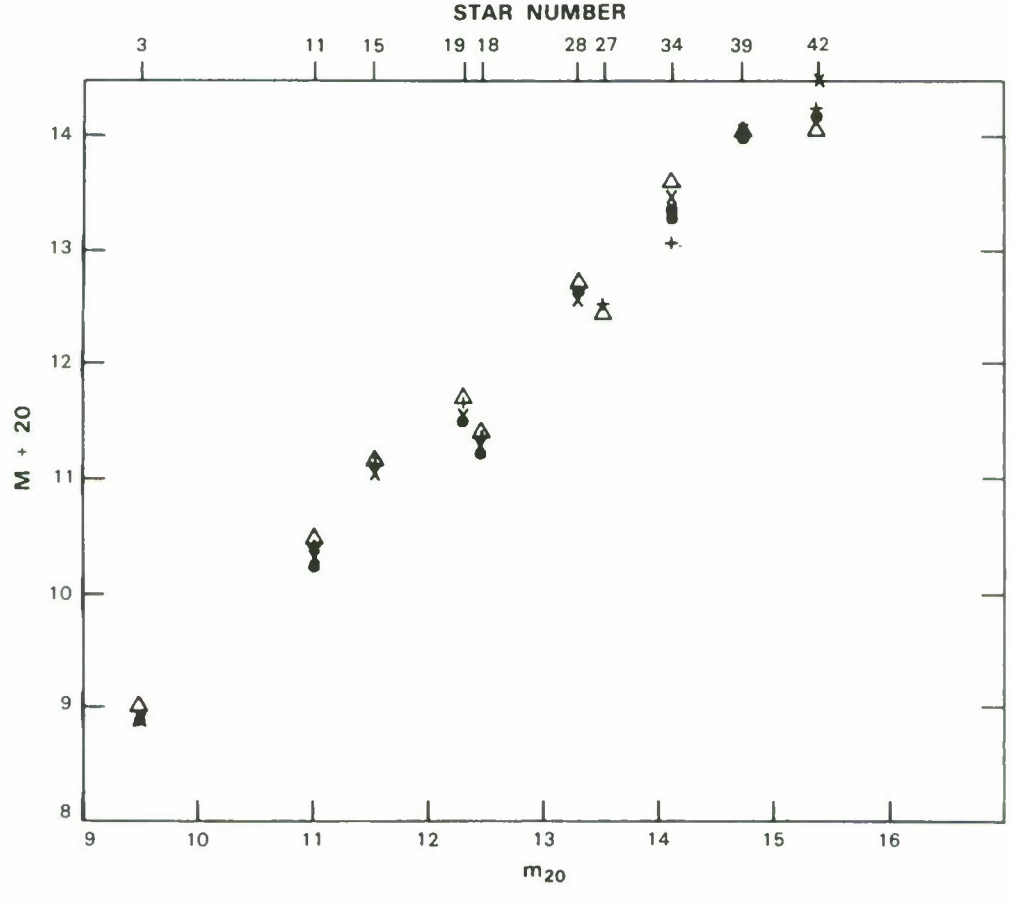

73765-5

Figure 5. A star-by-star and frame-by-frame graphical representation of the frame-to-frame variability for static stars. Note that the spread worsens as the stars get fainter.

TABLE 4

Least-Squares Parameters for Star Streak Heads*

Frame Number	a	b	Residual
1	1.08	$-20^{m}.57$	$0^{m}.21$
2	1.12	-21.05	0.12
3	1.30	-22.89	0.21
4	1.04	-20.17	0.18
5	1.17	-21.50	0.33
6	0.94	-19.08	0.28
All	1.11	-20.84	0.27

* $m = am_{20} + b$

TABLE 5

Least-Squares Parameters for Star Streak Heads*

Frame Number	a	b	c	Residual
1	$-20^{m}.82$	1.10	0.23	$0^{m}.18$
2	-21.55	1.12	0.77	0.14
3	-23.41	1.30	0.73	0.24
4	-21.59	1.20	-0.12	0.22
5	-21.51	1.19	-0.14	0.26
6	-20.38	1.06	0.15	0.11
All	-21.11	1.11	0.38	0.26

* $m = a + bV + c(B-V)$

B. Star Streak Heads

We have a total of six frames of star streak head data. This is summarized in Tables 4, 5, and Figure 6. These results are noticeably better than they would have been because we eliminated the brightest stars from the formal fitting process. Once again large frame-to-frame variations are present well above the system limiting magnitude. Note, too, that the faintest star for which we could successfully perform these measures is almost two magnitudes brighter than the faintest star for which we could successfully perform the preceding measures. This trend continues as we move on to streaks.

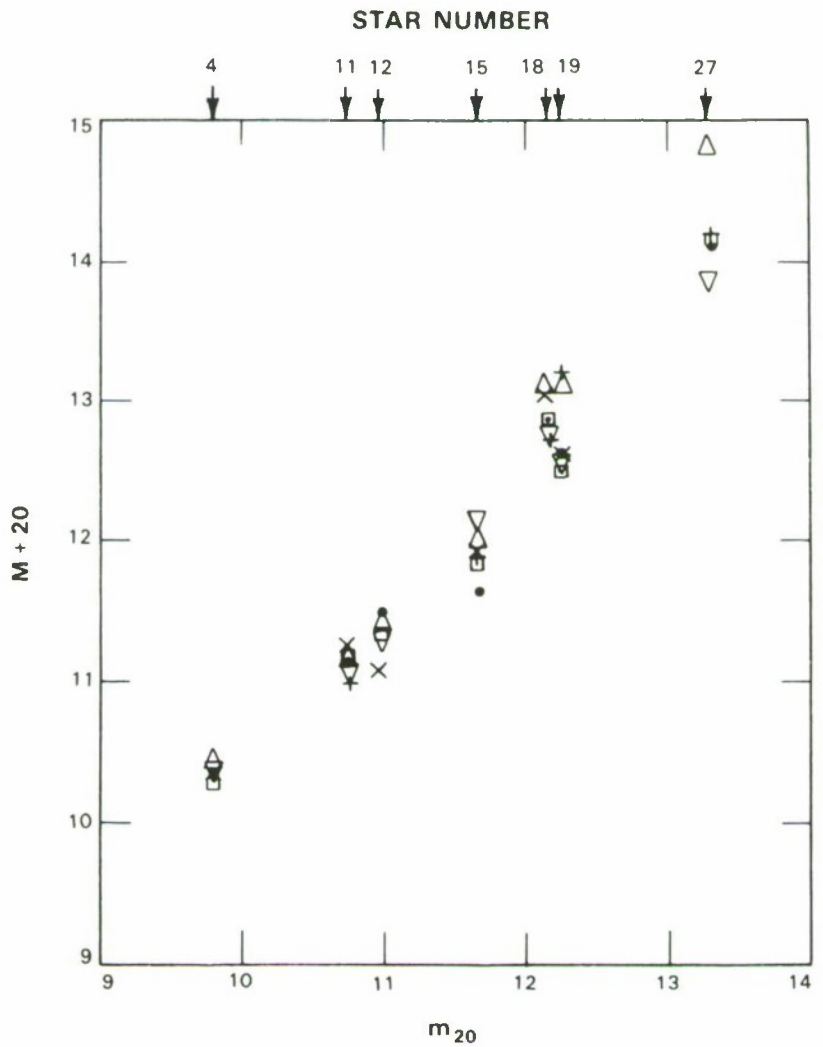

73765-1

Figure 6. A star-by-star and frame-by-frame graphical representation of the frame-to-frame variability for star streak heads. Note that the spread worsens as the stars get fainter.

C. Streaking Stars

Tables 6 and 7 are streaking star results in the same format as Tables 2 and 3. Neither has the amplitude of the zero point variation decreased nor has the color correction improved. Finally, there are fewer stars in these fits because of the inability to actually see (and therefore measure) their streaks. It should be clear from Figure 5 that the static star calibration is losing repeatability beyond 14^m, well above the static limiting magnitude of the system. It is even worse for streaking stars — the faintest star included is No. 25 ($m_{20} = 13^m.1$).

TABLE 6

Least-Squares Parameters for Streaking Stars*

Frame Number	a	b	Residual
1	1.06	$-21^m.58$	$0^m.18$
2	1.19	-23.11	0.27
All	1.13	-22.47	0.22

* $m = am_{20} + b$

TABLE 7

Least-Squares Parameters for Streaking Stars*

Frame Number	a	b	c	Residual
1	$-21^m.21$	1.03	0.03	$0^m.07$
2	-22.43	1.14	-0.10	0.18
All	-21.88	1.09	0.05	0.13

* $m = a + bV + c(B-V)$

D. Conclusions

We have made a reasonable attempt to try to photometrically calibrate streaks recorded on videotape at the ETS. We have included, at least to first-order, all extinction, color, camera target sensitivity variations, position angle of angular velocity, and so on, systematic effects. The result, even for brighter fixed (i.e., "static") stars, is that photometry to 0^m5 is not possible. For streaking stars at moderate near-Earth speeds, 0°42/s, our conclusions are even more pessimistic. While not discounting the possibility that we have missed something major, we do not see it. Nor do we believe that any complex of second-order effects is operating to vitiate what appears to be a straightforward procedure.

REPORT DOCUMENTATION PAGE		READ INSTRUCTIONS BEFORE COMPLETING FORM
1. REPORT NUMBER ESD-TR-86-005	2. GOVT ACCESSION NO.	3. RECIPIENT'S CATALOG NUMBER
4. TITLE *(and Subtitle)* Calibration of ETS Videotapes		5. TYPE OF REPORT & PERIOD COVERED Project Report 6. PERFORMING ORG. REPORT NUMBER Project Report ETS-77
7. AUTHOR*(s)* Anthony J. Yakutis, Laurence G. Taff, and Suzanne Sayer		8. CONTRACT OR GRANT NUMBER*(s)* F19628-85-C-0002
9. PERFORMING ORGANIZATION NAME AND ADDRESS Lincoln Laboratory, M.I.T. P.O. Box 73 Lexington, MA 02173-0073		10. PROGRAM ELEMENT, PROJECT, TASK AREA & WORK UNIT NUMBERS Program Element Nos. 63428F and 1242F Project Nos. 2698 and 2295
11. CONTROLLING OFFICE NAME AND ADDRESS Air Force Systems Command, USAF Andrews AFB Washington, DC 20334		12. REPORT DATE 29 April 1986 13. NUMBER OF PAGES 30
14. MONITORING AGENCY NAME & ADDRESS *(if different from Controlling Office)* Electronic Systems Division Hanscom AFB, MA 01731		15. SECURITY CLASS. *(of this Report)* Unclassified 15a. DECLASSIFICATION DOWNGRADING SCHEDULE

16. DISTRIBUTION STATEMENT *(of this Report)*

Approved for public release; distribution unlimited.

17. DISTRIBUTION STATEMENT *(of the abstract entered in Block 20, if different from Report)*

18. SUPPLEMENTARY NOTES

None

19. KEY WORDS *(Continue on reverse side if necessary and identify by block number)*

photometry calibration
artificial satellites
apparent magnitude
video observing
streak measurement

20. ABSTRACT *(Continue on reverse side if necessary and identify by block number)*

This Project Report discusses an attempt to calibrate photometric data acquired from streaks generated by moving objects which were observed at the ETS. This is desirable for both natural and artificial bodies. The utility of a meaningful apparent magnitude from streak data would allow statistical studies of size-albedo distributions, serve as a size indicator in the absence of traditional photometry, and alleviate the difficulties of artificial satellite photometry on the rapidly moving near-Earth population. Unfortunately we have been unsuccessful at this endeavor. Moreover, were this trial successful we can envisage sundry systematic errors that would creep into more widespread applications. Some of these are related to angular speed, field of view, time duration of a streak, frame-to-frame variability, length of streak arc across the field of view, and the angle between the angular velocity and the direction of the video scan lines. This general topic is important and we will pursue other approaches if they can address our apprehensions.